

Self-assembly of aromatic biscarbamate gelators: effect of spacer length on the gelation and rheology

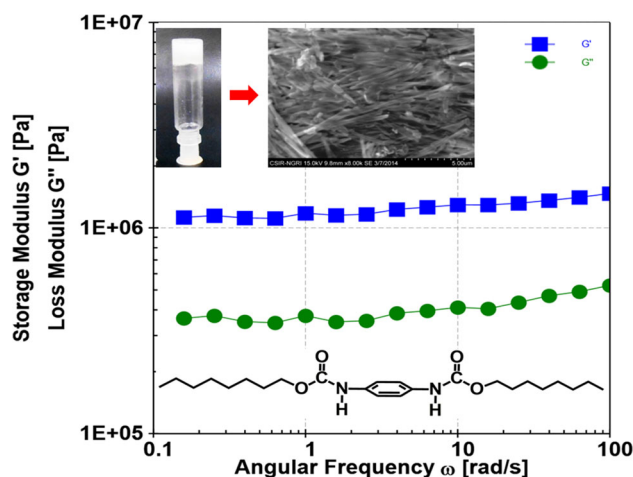
Sravan baddi¹ · D. Srinivasa Sarma² · Aruna Palanisamy¹

Received: 30 October 2015 / Accepted: 30 March 2016 / Published online: 21 April 2016
© Springer Science+Business Media New York 2016

Abstract Low molecular weight biscarbamate organogelators (LMWBGs) with simple molecular structures that could gel different types of organic solvents were synthesized. The LMWBGs were composed of a long hydrophobic tail of linear fatty alcohol (C_8 – C_{18}) and an aromatic core and could gel organic solvents such as xylene, toluene, NMP, cyclohexanol and chlorobenzene at a concentration of 10–15 mg/mL. Gelation studies indicated that the alkyl chain length residues did not affect the gelation time which was generally around 10–15 min leading to opaque gels in all the solvents. The gels in *p*-xylene were studied by FTIR spectroscopy and differential scanning calorimetry (DSC) for the nature of the interactions between the gelators and the solvent. FTIR spectroscopic studies revealed that hydrogen bonding and van der Waals interactions were the driving forces for the formation of the gels, while solid-state UV–visible studies revealed the existence of π – π interaction in the xerogel. The gel melting temperatures were found to decrease and then increase with increasing alkyl chain length as observed in DSC. The microscopic observations (FE-SEM) suggested that the gelator molecules self-assembled leading to nano- and microfibrils in the turbid gel, and as the alkyl chain length increased, the width of the fibrils increased. Rheological studies evinced the viscoelastic nature of the soft gels

viscoelasticity increased with increasing gelator concentration, while fluidity increased with increasing chain length. The X-ray diffraction analysis revealed that in the xerogels from *p*-xylene the molecules aggregated into a layered structure. This study on the influence of alkyl side chains shows that hydrogen bonding and van der Waals interactions play a significant role in the morphology of such self-assembled structures.

Graphical Abstract



Electronic supplementary material The online version of this article (doi:10.1007/s10971-016-4036-x) contains supplementary material, which is available to authorized users.

✉ Aruna Palanisamy
aruna@iict.res.in; arunap73@rediffmail.com

¹ Polymers and Functional Materials Division, Indian Institute of Chemical Technology (CSIR-IICT), Hyderabad, India

² Geochemistry Division, National Geophysical Research Institute (CSIR-NGRI), Hyderabad, India

Keywords Self-assembly · Gelators · Gelation · Xerogels · Microfibrils · Hydrogen bonding

1 Introduction

Most of the low molecular weight gelators so far reported have not been found by any design principle but by serendipity. Hence, the designing of new novel gelators is a

challenging goal [1–3]. Low molecular weight gelators and their gelation phenomenon is branch of supra-molecular chemistry which concentrates on weaker and reversible non-covalent interactions between molecules [4]. These gelator molecules self-assemble in organic solvents or water through interactions, such as hydrogen bonding, hydrophobic interactions, polar–polar interactions, electrostatic interactions and π – π stacking. These forces drive the one-dimensional growth of the gelator molecules leading to nanoscale or microscale structures in the form of, fibres, strands and tapes which may sometimes later join together to form three-dimensional networks [5–8]. Among the various non-covalent interactions, hydrogen bond-mediated self-assembly has been studied extensively [9–15]. For molecules to exhibit enhanced H bonding, one needs to design molecules in such a way that there is an ordered arrangement of the molecules in 3D [16, 17]. An appropriate design of molecules with hydrogen bonding moieties leads to molecular self-assembly, but morphology of the structures depends on the secondary non-covalent interactions such as van der Waals forces. Sundarajan et al. have investigated the influence of side chain length as well as single versus double hydrogen bond motifs on the morphology and miscibility behaviour upon crystallization, blending, and gelation of a class of hydrogen bond-mediated self-assembling aliphatic system of carbamates and biscarbamates [18]. Most of the reported organogels from LMWBGs have been thermoreversible, i.e. these gels can be easily transformed into solution by heating and back to gels by cooling the solutions above and below their sol–gel transition temperature [5] (sol–gel transition temperature). This reversible property of the gels can be used for controlled release of drugs in biomedical application, electronics/photonic materials, light harvesting systems, sensing materials, liquid crystal and fuel engineering [19–22].

To our knowledge, studies on the effect of alkyl chain length on the gelation behaviour of biscarbamates with aromatic core have not been reported so far. Earlier, we have synthesized low molecular weight biscarbamate organogelators (LMWBGs) with simple molecular structures. The LMBWGs were composed of a long hydrophobic tail of linear fatty alcohol (BG₈–BG₁₈) and an aromatic core that could gel organic solvents such as xylene, toluene, NMP, cyclohexanol and chlorobenzene at a concentration of 10–15 mg/mL. In addition, the gelators were capable of gelling ionic liquid (1, 3-di-n-butylimidazolium bromide) and one of the gelators (BG₁₂) was found to be very efficient. At a concentration of 30 mg/mL in ionic liquid, the gel exhibited good ionic conductivity. The specific capacity of the gelatinized electrolyte-based Mg-ion battery was 100 mAhg⁻¹, and the cycle life studies (500 cycles) indicated a stabilized discharge curve at 1.8 V at constant current

discharge of 0.1 mAcm⁻². Further information is available in our paper recently published [23]. In the present study, we have discussed (1) gelation of bicarbamates in different solvents, (2) gel properties and (3) influence of the alkyl side chains and hence the secondary forces on the spectral, morphological and thermal behaviour of these biscarbamate-based organogels which contain two hydrogen bonding motifs separated by benzene ring.

2 Experimental section

2.1 Materials

1-Octanol, 1-decanol, 1-dodecanol, 1-tetradecanol, 1-hexadecanol, 1-octadecanol, tetrahydrofuran (THF), dry dimethylformamide (DMF), methanol, (SDFCL-Hyderabad, India), 1, 4-phenylene diisocyanate and DBTDL (Sigma-Aldrich) were used as such.

2.2 Techniques

¹H-NMR spectra were recorded in DMSO-d₆ on Bruker 500 MHz NMR spectrometer, and TMS was used as an internal reference. The nature of the gelator solvent interaction was determined by IR spectroscopy using Perkin-Elmer, spectrum 100 FTIR spectrometer. The gel and the solution of the gelator in a specific solvent were sandwiched between KBr discs and scanned in the 4000–400 cm⁻¹ range. The gel melting temperatures were determined by DSC Q 100 series (TA instruments) from room temperature to 140 °C at a heating rate of 5 °C/min under nitrogen atmosphere (flow rate 50 ml/min). Weighed quantity of the gel (10 mg) was taken in a hermetic pan and sealed. The xerogel for XRD and SEM was obtained by freeze drying the gels (in *p*-xylene) at –100 °C. X-ray diffraction spectra for the xerogels were obtained by using a Siemens/D-5000 X-ray diffractometer using Cu K α radiation of wavelength 1.54 Å and continuous scan speed of 0.045/min. Diffraction data were recorded at room temperature, in the range of 2° ≤ 2θ ≤ 65°. The crystallite size, *L*, corresponding to a particular reflection (*d* spacing's of 4.6 and 3.7 Å) was calculated by the Scherrer equation: [24, 25].

$$\text{Crystallite size} = \frac{K\lambda}{\beta \cos\theta} \quad (1)$$

where λ is wavelength of the X-ray (in nm), θ is half the scattering angle, β is the half width of the peak on the 2 θ scale in radians and $K = 0.9$. And SEM images of the xerogels were taken on scanning electron microscope–energy-dispersive spectrometer (SEM–EDS), HITACHI S-3400 N. The accelerating voltage was 15 kV, and the

emission was 10 mA. The UV–Vis absorption spectra were obtained using a UV–Vis–NIR-3600 Spectrophotometer, Shimadzu, Japan. All spectra were recorded in powder state (xerogels from *p*-xylene) at room temperature, and the excitation wavelengths of the spectra were 200–600 nm. Rheological measurements were taken with a strain-controlled rheometer (series Modular Compact Rheometer 102, Anton Paar's, Graz, Austria, Europe) equipped with a parallel plate. The gap distance was fixed at 1 mm. To determine the storage moduli, G' and loss moduli, G'' , the measured angular frequency, ω , ranged from 0.1 to 100 s^{-1} and the applied shear strain amplitude was 0.5 % in the linear viscoelastic regime measured at room temperature (25 °C), and at the same time, the strain amplitude sweep was performed at a constant frequency (f) 1.0 Hz with strain ranging from 0.01 to 100, at 25 °C.

2.3 Gelation test

A known weight of gelator was mixed with a 1 mL of organic solvent in a sealed test tube, and the mixture was heated until the solid dissolved; then, the resulting solution was cooled to room temperature and the gelation was checked visually by test-tube inversion method. Gelation was considered to have occurred when a homogenous substance was obtained which exhibited no gravitational flow, and it was denoted as 'G'. In some cases, solution and solid-like gel may coexist within a system. This kind of system has been referred to as 'partial gels (PG)'. For systems, in which only solution remained until the end of the tests, they were referred to as solution (S). For systems, which are clear solutions when they are hot, but precipitation occurs when they are cooled down to room temperature, these systems are denoted by 'P (Precipitation)'. The system, in which the potential gelator could not be dissolved even at the boiling point of the solvent, was called an insoluble system (I) [26–28].

3 Results and discussion

3.1 Synthesis of gelator

The fatty alcohols (C_8 – C_{18}) were dissolved in 10 mL of dry DMF taken in a 100-ml RB flask, and PDI (dissolved in dry DMF) was added drop wise to the solution at room temperature. DBTDL (0.01 % by weight) was added to catalyse the reaction. The ratio of 1, 4-phenylene diisocyanate to alcohol was taken as 1:2.2 eqv. The temperature was then raised to 60 °C and continued for 2 h under the nitrogen atmosphere, and the reaction was monitored by TLC. The final compound was isolated by precipitating the reaction mixture in excess of water followed by filtering it.

The precipitate was dried and unreacted alcohol was removed by washing the product in methanol wherein the unreacted alcohol dissolved in methanol, then recrystallized from THF and dried under vacuum. Structure of the gelators was confirmed by $^1\text{H-NMR}$ (see supplementary information Fig.S1) (Scheme 1).

3.2 Gelation behaviour

The gelation abilities of the six types of gelator compounds (BG_8 – BG_{18}) were tested in different organic solvents among which xylene, toluene, NMP, cyclohexanol and chlorobenzene showed gelation at a concentration of 10–15 mg/ml. Gels appeared to be turbid (Fig. 1a) at all concentrations irrespective of the nature of the solvent. The time of gelation varied between 5–10 min depending on the nature of solvent. The gelation time in toluene and xylene was found to be 5 and 8 min, whereas in cyclohexanol, chlorobenzene and NMP, it was ~ 10 min. The time of gelation did not vary with the alkyl chain length. The alkyl units favour dissolution of the gelator compound in hydrophobic solvents. The aromatic solvents containing alkyl or halogen group attached to it were found to be preferably trapped by the gelators. This could be due to the hydrophobic nature of aromatic solvents towards the hydrophilic functional groups, such as amides. The studies with *o*-xylene, *m*-xylene and *p*-xylene indicate that the position of methyl does not have significant effect on MGC. Among all the solvents studied, *p*-xylene is found to be the best solvent for gelation. This could be due to the match in the symmetries of gelator and *p*-xylene. The results are summarized in Table 1.

The biscarbamate gels were found to be stable at room temperature for five to six months (under sealed conditions). In all the cases, the gels showed thermoreversibility as shown in Fig. 1b. The thermal stability of the organogels was investigated by measuring the gel–sol transition temperature (T_{gel}) both manually and by using DSC. In the present study, the alkyl chain length was varied using a specific solvent at a fixed concentration (*p*-xylene, 15 mg/mL). The gel melting temperatures (listed in Table 3) were determined manually by heating the sample vial in the temperature controlled bath at 5 °C/min until tube inversion showed that the gel had melted. When the alkyl chain length increased from BG_8 to BG_{18} , the gel melting was found to increase from 83 to 105 °C. To study the effect of concentration, the BG_8 gels were prepared in *p*-xylene at various concentrations (15, 30 and 45 mg/mL). When the concentration was increased from 15 to 45 mg/mL, the gel melting point increased from 83 to 105 °C and the time of gelation decreased from 8 to 4 min. Such an increase in T_{gel} may be attributed to increased non-covalent

Scheme 1 Schematic representation of the synthesis of the biscarbamate gelators

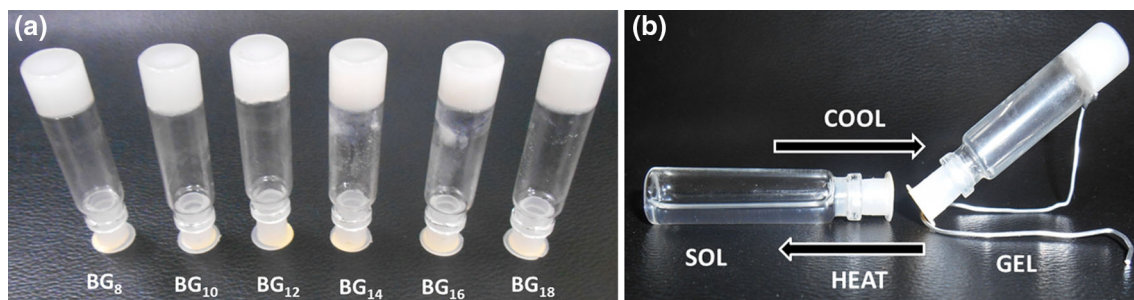
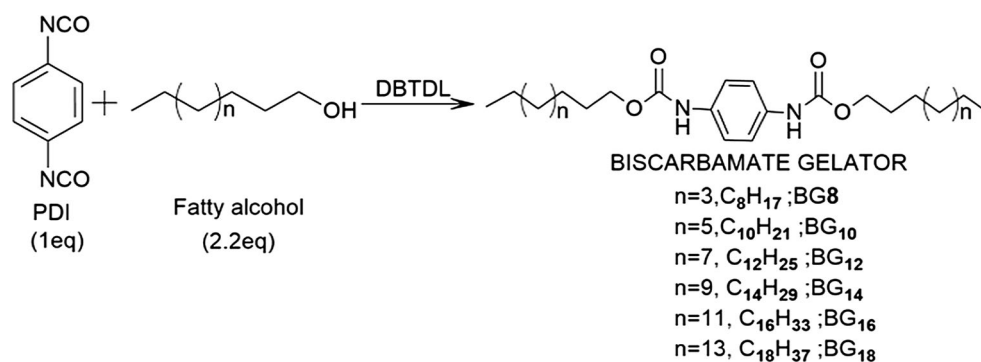


Fig. 1 **a** Image of gels from BG₈–BG₁₈ and **b** illustrations depicting the thermoreversibility of the gelators (in *p*-xylene) by inverted vial method

Table 1 Gelation properties and minimum gelation concentration (MGC) of the biscarbamate compounds of varying chain length in organic solvents

Solvent	BG ₈	BG ₁₀	BG ₁₂	BG ₁₄	BG ₁₆	BG ₁₈
Dioxane	P	P	P	P	P	P
Toluene	G(12)	G(10)	G(12)	PG(15)	G(14)	G(12)
Benzene	P	P	P	P	P	P
NMP	PG(15)	PG(15)	PG(15)	PG(15)	G(15)	G(15)
THF	P	P	P	P	P	P
Butanol	P	P	P	P	P	P
Cyclohexanol	PG(15)	PG(15)	G(15)	PG(15)	G(15)	G(15)
Ethyl acetate	P	P	P	P	P	P
Acetone	P	P	P	P	P	P
Chloroform	I	I	I	I	I	I
<i>o</i> -Xylene	G(10)	G(10)	G(15)	G(15)	G(10)	G(10)
<i>m</i> -Xylene	G(10)	G(10)	G(15)	G(15)	G(10)	G(10)
DMF	S	S	S	S	S	S
<i>p</i> -Xylene	G(10)	G(10)	G(15)	G(15)	G(10)	G(10)
DMAc	S	S	S	S	S	S
DMSO	S	S	S	S	S	S

Number within parenthesis indicates the minimum concentration of the gelator required for gelation (MGC, mg/mL)

G Stable gel formed at RT; PG partial gel consisting of gel and solution; P precipitate after dissolution; S solution; I insoluble system

interactions such as hydrogen bonding and hydrophobic interactions that are responsible for forming self-assembled structures in the gels [19, 29, 30].

3.3 FTIR spectroscopy

FTIR measurements can provide useful information for confirming hydrogen bonding and van der Waals interactions. Accordingly, the FTIR spectra of BG₈–BG₁₈ gelators in gel and solution state were recorded in *p*-xylene. From the spectrum of the control, it can be observed that the typical bands of BG₈-gelator in solution and gel state (Fig. 2) corresponding to the stretching and bending vibrations of NH appeared at 3326 cm⁻¹ (ν_{N-H} stretch), 1516 cm⁻¹ (ν_{N-H} bend) and 1693 cm⁻¹ (ν_{C=O} of amide), respectively. Upon gelation, the bands shifted to 3308 cm⁻¹ (ν_{N-H} stretch), 1515 cm⁻¹ (ν_{N-H} bend) and 1687 cm⁻¹ (ν_{C=O} of amide), respectively. This is an evidence for the participation of the NH group in the formation of hydrogen bonds, which should be one of the driving forces for the formation of the gel. The presence of two amide moieties can drive the aggregate formation through amide-to-amide N–H...O hydrogen bonding. Table 2 shows that the peak intensity of H-bonded N–H and C=O bands increase slightly from BG₈ to BG₁₂ and then decreases with further increase in the length of alkyl side chain.

The asymmetric and symmetric stretching frequencies (ν_{asym} and ν_{sym}) were 2923 and 2868 cm⁻¹ corresponding to solution, and 2968 cm⁻¹ corresponds to gel state. The peak corresponding to the asymmetric stretching appears to be broad, and the symmetric stretching frequency disappeared in gel state. The spectra of gels Fig.S2 (supporting information) showed an increase in the asymmetric

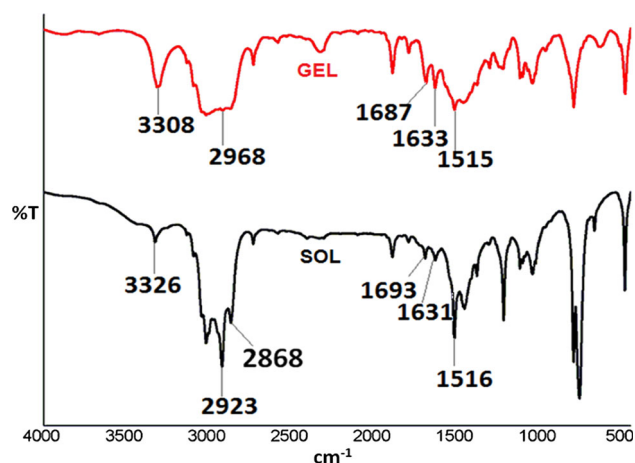


Fig. 2 Solvent subtracted FTIR spectra of BG₈ gelator in *p*-xylene (15 mg/ml) solution and gel state

absorption frequency, but from BG₈–BG₁₈ gels the absorption frequency of the asymmetric CH₂ vibration decreased with increasing alkyl chain length, indicating an increase in van der Waals interactions. Such a type of interaction leads to the formation of short thick fibre-like morphology in a turbid gel. NH-stretching frequencies (3308–3325 cm⁻¹) shifted to higher wave numbers, and

CH₂-stretching frequencies (2968–2921 cm⁻¹) shifted to lower wave numbers from BG₈ to BG₁₈ gels (Table 2). This is because, in BG₈, chain length is less and hence hydrogen bonding predominates, but in the case of BG₁₈, the chain being longer facilitates van der Waals interactions to hydrogen bonding. Since the number of the H bonds remains constant even with increasing chain length and only the extent of the van der Waals interaction changes, beyond a certain chain length, the van der Waals forces predominate.

3.4 Thermal behaviour

The thermal behaviour of the biscarbamate gel systems was investigated by differential scanning calorimetry (DSC) in *p*-xylene, due to its high boiling point and its ability to form gels with all the compounds in the series. In the first heating cycle, these gels showed two types of endothermic transitions: first transition corresponds to pre-melting, and second transition corresponds to actual melting of gel (T_{gel}) (Table 3). The melting points of the gels (defined as the temperature above which macroscopic flow appears) were also determined by visually monitoring the flow of the gels in a thermally controlled bath which showed that the sharp

Table 2 Selected FTIR absorption bands for the N–H, C=O and C–H groups for the biscarbamates with different alkyl chain lengths

Sample description	H-bonded N–H stretch		H-bonded C=O stretch		N–H bend	CH ₂ stretch
	Peak position (cm ⁻¹)	Intensity	Peak position (cm ⁻¹)	Intensity		
BG ₈	3308	89	1687	90	1515	2968
BG ₁₀	3308	92	1690	92	1514	2965
BG ₁₂	3315	94	1692	95	1514	2963
BG ₁₄	3315	75	1690	74	1514	2928
BG ₁₆	3325	69	1693	74	1516	2922
BG ₁₈	3325	63	1694	70	1514	2921

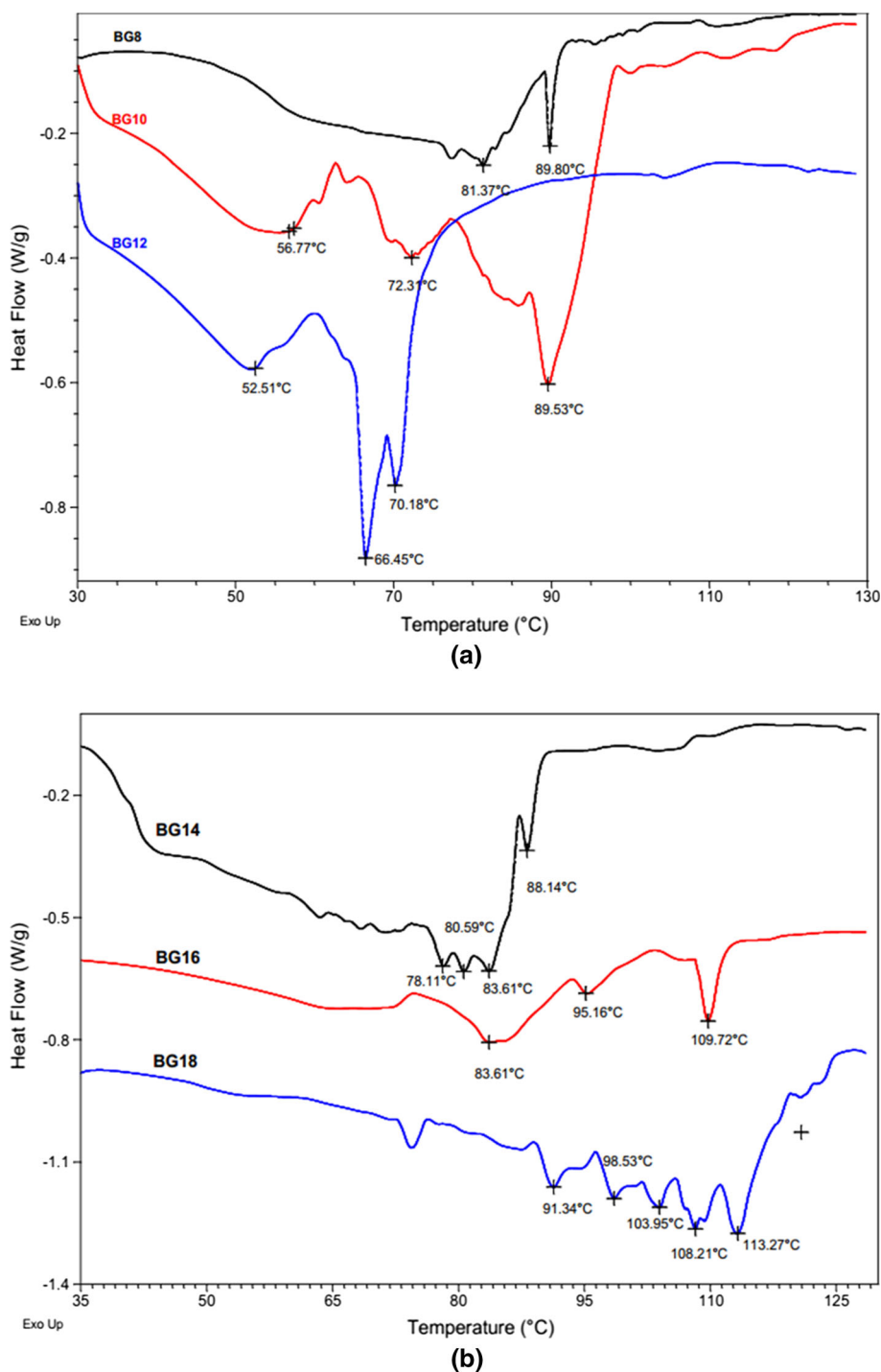
Table 3 Thermal properties of the gelators and gels in *p*-xylene

Alkyl chain length	MP	$T_{\text{gel}}^{\text{a}}$	DSC transitions (°C)		Concentration variation of BG ₈ gelator				
			Premelting peaks	T_{gel}	Conc (mg/mL)	G_{T}	$T_{\text{gel}}^{\text{al}}$	DSC transition (°C)	
								Premelting	T_{gel}
BG ₈	153.0	83	81.3	89.8	15	8	83	81.3	89.8
BG ₁₀	151.0	80	56.7/72.3	89.5					
BG ₁₂	149.5	65	52.1/66.4	70.1	30	5	95	86.3	106.6
BG ₁₄	149.4	83	80.5/83.6	88.1					
BG ₁₆	148.7	95	83.6/95.1	109.7	45	4	105	101.6	112.7
BG ₁₈	148.1	105	92.3/98.5/108.2	113.2					

MP Melting point of gelator (°C), T_{gel} Melting points of gels (°C), G_{T} Time of gelation (min)

^a Concentration: 15 mg/mL; Melting points determined by heating the sample vial in the temperature controlled bath until tube inversion showed that the gel had melted

Fig. 3 **a** DSC curves of BG₈–BG₁₂ gelators in *p*-xylene at a concentration of 15 mg/mL and **b** DSC curves of BG₁₄–BG₁₈ gelators in *p*-xylene at a concentration of 15 mg/mL



transitions in the thermogram corresponds to the actual melting of the gel. At the temperatures of the broad transitions, there is no visual change in the gels at macroscopic level. The cooling curves of the molten gels exhibited an exotherm (fig.S3a) which corresponds to the sol → gel transition confirming the thermoreversible nature of the gels.

The DSC curves of the BG₈–BG₁₈ gels (Fig. 3a, b) showed two to three transitions in the first heating, BG₈ gel

showing two endothermic peaks located at 81.37 and 89.80 °C, respectively. The broad endotherm at 81.37 °C can be ascribed to the pre-melting of the gel, and the sharp endotherm at 89.80 °C can be ascribed to the actual melting of main constituent indicating the phase transition temperature of the gel to sol. An explanation for the appearance of these pre-melting transitions is partial melting of the gelator network. It can be assumed that the

3D array of the microfibrils collapses before the single fibres start to break down [31–33]. From Fig. 3a, BG₈ to BG₁₂ T_{gel} decreased from 89.80 to 70.18 °C. In BG₈ gel, hydrogen bonding is predominant over van der Waals interaction, whereas in BG₁₂ gel the hydrogen bonding and van der Waal forces are balanced. As the chain length further increased from BG₁₄ to BG₁₈, the gels showed three endothermic transition peaks upon heating: two broad transitions and one sharp peak as shown in Fig. 3b. The endothermic transitions shifted from 88.14 to 113.27 °C wherein the van der Waals forces predominate hydrogen bonding at higher alkyl chain lengths.

BG₈ gelator in *p*-xylene was chosen to study the effect of concentration on the gel properties. When the gelator concentration increased from 15 to 45 mg/mL, the peaks shifted to higher temperatures as shown in Fig. S3b (Supporting information) and listed in Table 3. With shorter alkyl side chains (BG₈), the hydrogen bonding interaction would predominate the van der Waals interaction. With the long alkyl side chains (BG₁₈), the van der Waals interactions would become significant, while the extent of hydrogen bonding remains same. At intermediate lengths, (BG₁₂), there would be a balance between the two. Due to this reason, the melting points of the gels initially showed a decreasing trend and later an increasing trend.

3.5 Rheological studies

In the rheological measurements (Fig. 4), the gel samples were deformed sinusoidally to give the storage modulus (G') and loss modulus (G''). The storage modulus and loss modulus were measured as a function of angular frequency (ω), at room temperature. During the oscillation frequency sweep test [34–36], both G' and G'' values of the gel samples were weakly depending on the frequency and all gels have their storage moduli G' greater than loss moduli

G'' ; this rheological behaviour evidenced the viscoelastic nature of the soft elastic gels. This suggests that there had been no phase transition during the frequency sweep process and the gel possesses good tolerance to external forces and can be considered as satisfactory colloidal materials. The results are shown in Fig. 4. Comparison of the G' and complex viscosity (η^*) values of the gels indicates that the G' and η^* of a gel decrease with increasing chain length of the gelator from BG₈ to BG₁₂ (Fig. 4a and 5a) and then increase from BG₁₄ to BG₁₈ (Fig. 4b and 5b). To further elucidate the importance of gelator concentration to the rheological properties of a supramolecular gel, the G' values of BG₈ in *p*-xylene at different concentrations (15, 30 and 45 mg/mL) are measured as a function of angular frequency and the results are shown in Fig. 4c and 5c. It can be seen that the value of G' and η^* increases with the gelator concentration [37], indicating that both the stability of the gel network and the elastic property of the gel depend upon the concentration of the gelator in the solvent. This confirms the gel structure which is not very clear in DSC measurements.

To investigate the effects of alkyl chain length and concentration of gelator on the mechanical properties of the gels, the storage modulus G' and loss modulus G'' of the gel systems were measured as functions of shear stress (τ) at a constant frequency (f) of 1.0 Hz at 25 °C [28, 38]. From Fig. 6a, it can be seen that the value of G' is much larger than the value of G'' with the small shear force at the beginning, suggesting the stability and the dominant elastic nature of the gel. Both G' and G'' remain almost unchanged with the increase in the shear stress, and in a definite stress value, they cross each other, and finally, the G'' value is greater than G' after a critical shear stress, revealing the collapse of the 3D gel networks and the dominant fluid character of the organogel. This critical stress value is referred to as yield stress (τ_y). From

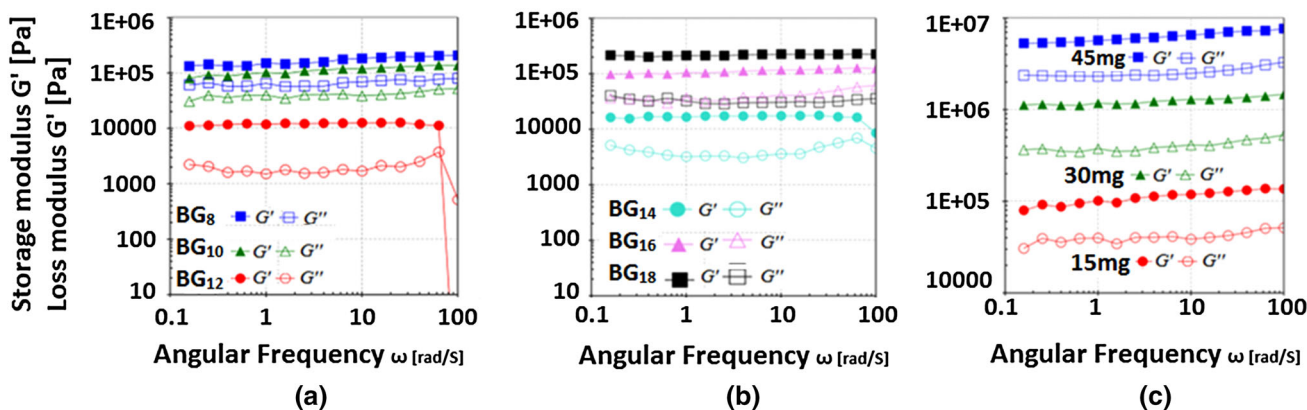


Fig. 4 a Evolution of G' and G'' as a function of the angular frequency of BG₈–BG₁₂ gels in *p*-xylene at 15 mg/mL. b Evolution of G' and G'' as a function of the angular frequency of BG₁₄–BG₁₈ gels

in *p*-xylene at 15 mg/mL. c Evolution of G' and G'' as a function of the angular frequency at different concentrations (15, 30 and 45 mg/mL) of BG₈ gel in *p*-xylene

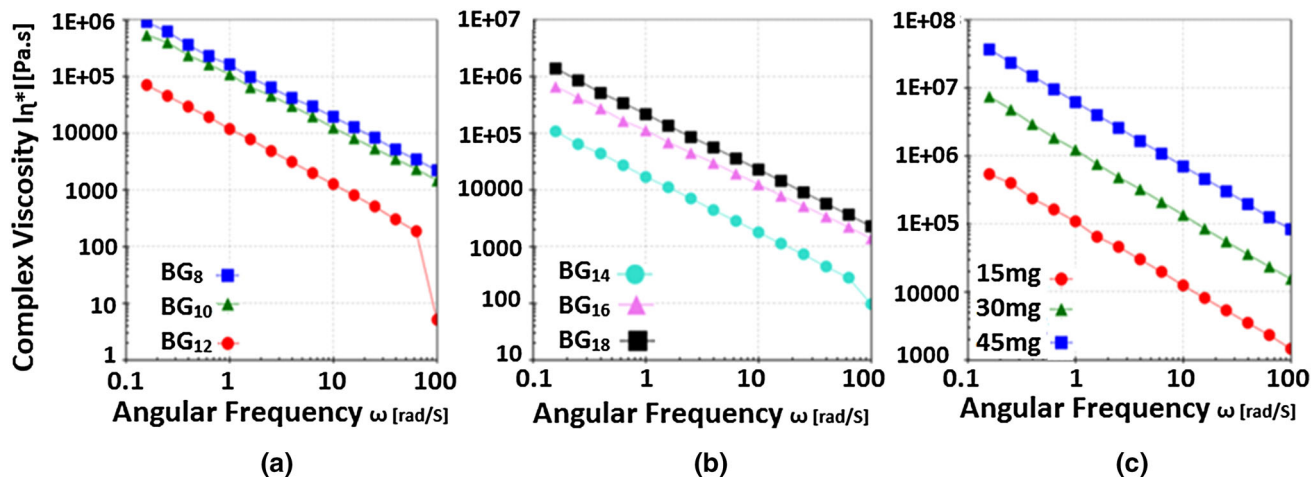


Fig. 5 **a** The evolution of complex viscosity as a function of angular frequency of BG₈–BG₁₂ gels, **b** the evolution of complex viscosity as a function of angular frequency of BG₁₄–BG₁₈ gels and **c** the

evolution of complex viscosity as a function of angular frequency of BG₈ gel at different concentrations (15, 30 and 45 mg/mL) in *p*-xylene

Fig. 6 **a** Evolution of G' as a function of applied shear stress of BG₈–BG₁₈ gels at 15 mg/mL concentration in *p*-xylene and **b** evolution of G' as a function of applied shear stress at different concentrations of BG₈ gel in *p*-xylene

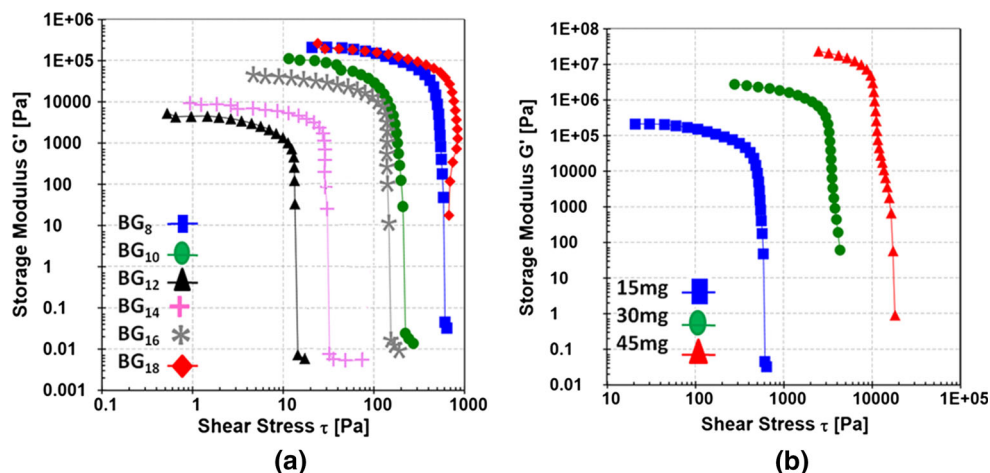


figure and table, the G' and τ_y of the gels well depend upon the alkyl chain lengths of the gelator molecules. It is seen that the G' and τ_y values decrease with increasing chain length from BG₈ to BG₁₂ and then increase with increasing chain length from BG₁₄ to BG₁₈. BG₁₂ shows lower yield stress indicating that the gel has less strength, while BG₁₈ shows higher yield stress and hence stiff gels. These results demonstrate clearly that the alkyl chain length of the gelators has a significant effect upon the mechanical properties of the resulting gels. Figure 6b and Table 4 demonstrate that the yield stress increases with increasing concentration of the gelator. These results suggest that the stability of the 3D gel network depends upon the concentration of the gelator and the viscoelasticity of the gel is enhanced with increasing gelator concentration. G' and G'' versus strain graphs of gels at all variations are shown in figure S4 and S5. All these results

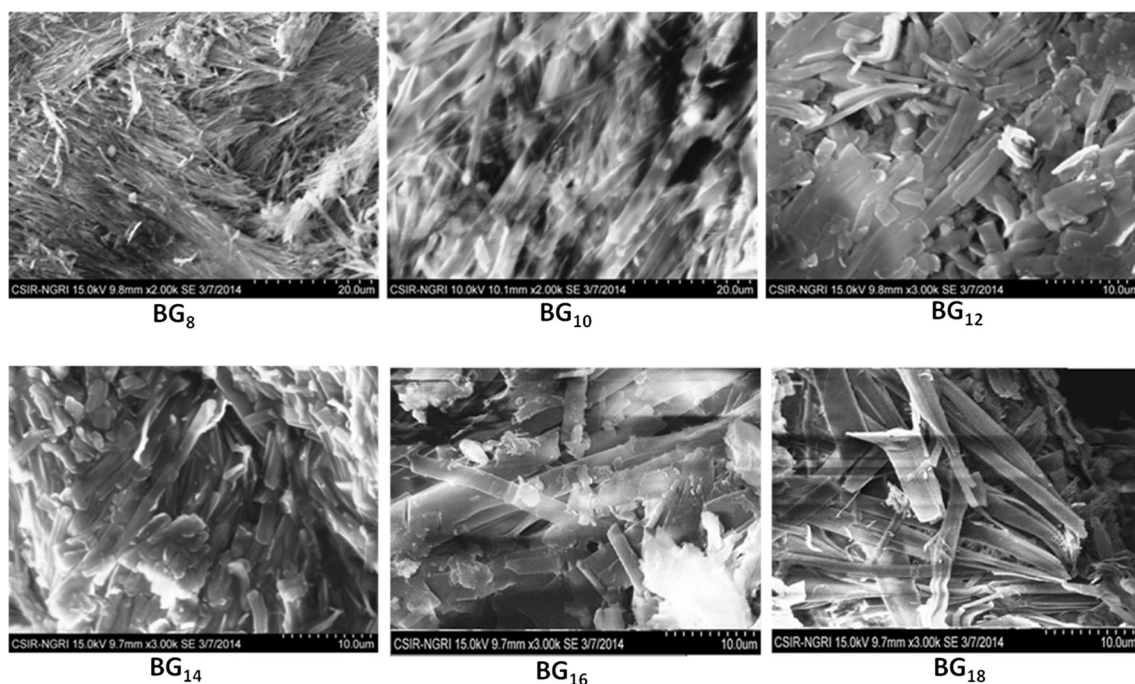
are consistent with the previous T_{gel} values (dropping ball method and DSC) determined for gel samples.

3.6 Microstructure

The morphology (nano-/microstructures formed at the microlevel) of the xerogels of the gelators in *p*-xylene was investigated by FE-SEM. This technique is a tool to assess the impact of the alkyl unit on the mode of self-assembly. The morphology of BG₈–BG₁₆ xerogels shows fibres, whereas BG₁₈ shows tape-like morphology (Fig. 7). Interestingly, changing the length of the alkyl chain impacts a significant morphological change. Thin fibres were observed in BG₈ (302–372 nm), BG₁₀ (1.2–1.4 μm), BG₁₂ (1.45–1.75 μm), BG₁₄ (1.7–1.9 μm) and BG₁₆ (2.2–2.7 μm and 3.7–4.7 μm) xerogels (width of the fibre indicated within the parenthesis), which self-assemble to

Table 4 Maximum storage modulus (G') and yield stress (τ_y) of BG₈–BG₁₈ gels at 15 mg/mL concentration and different concentrations of BG₈ gel in p-xylene

Sample name	G'	τ_y	Concentration variation BG ₈ gel		
			Concentration (mg)	G'	τ_y
BG ₈	2.093E + 05	610	15	2.093 + E05	610
BG ₁₀	1.1158 + 05	222			
BG ₁₂	5778	14	30	2.793 + E06	4335
BG ₁₄	9084	32			
BG ₁₆	46566	154	45	2.350 + E07	18,218
BG ₁₈	2.6048 + 05	674			

**Fig. 7** FE-SEM images of the xerogels of BG₈, BG₁₀, BG₁₂, BG₁₄, BG₁₆ and BG₁₈ gelators

form a bundle of fibres. The regular shape and high aspect ratio of the fibres are indicative of unidirectional stacking of gelator units resulting in a one-dimensional mode of self-assembly. Therefore, we assume that there is one-dimensional stacking of gelator units into fibres, which aggregates further into bundles, and that this process immobilizes the organic solvent, thus inducing gelation. BG₁₆ xerogel showed long tape-like morphology in addition to fibres (Fig S6a and d). BG₁₈ xerogel showed a tape-like morphology which is quite different from others, the width being 4.8–5.13 μm range. SEM studies revealed that the self-assembly of BG₈–BG₁₈ gels is driven by strongly directional intermolecular interactions. As the length of the alkyl chain increases, the molecular stacking of the gel fibres increases due to the contribution of the van der

Waals interaction relative to the hydrogen bond, and width of the fibre increases too.

3.7 UV–visible spectroscopy

Figure 8 shows the UV–visible absorption spectra of gelator and xerogel state. The three absorption peaks at 240, 280 (C=O) and 330 nm (π - π) correspond to the gelator, which were shifted to longer wavelengths, viz. 250, 292 and 390 nm in the xerogel. This red shift indicates the formation of J-aggregate in the xerogel; however, not much variation in the position of the peaks corresponding to the xerogels of varying chain length was observed. On the basis of these results, we can conclude that the π - π stacking of benzene rings together with the intermolecular

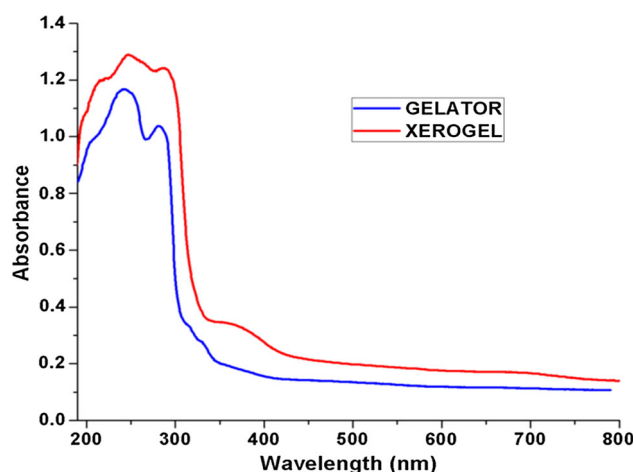


Fig. 8 UV-visible absorption of BG₈ gelator and xerogel (15 mg/mL in *p*-xylene) state

H bonding is responsible for the self-assembly leading to gel formation [39–43] (Fig. 9a).

3.8 XRD

In order to reveal the molecular packing of the biscarbamate gelators, the xerogels (BG₈–BG₁₈) were investigated by XRD technique. It is supposed that the XRD data came from the elemental fibres of the aggregates of the gelator molecules. The xerogels show a series of intense reflections in the $2\theta = 20\text{--}25^\circ$ range shown in Table S1 and Fig. 10a, b, which indicates the layered structure of the molecules in the gel fibres. All the biscarbamates show a common reflection with d spacing of 4.6 Å ($2\theta = 19.22^\circ$) and 3.7 Å

($2\theta = 23.46^\circ$), and the distance between the alkyl chains in this model is 4.6 Å; this d spacing thus corresponds to the plane of hydrogen bonding. These reflections were assigned to the distance between molecules forming the hydrogen bond and the growth direction of the short fibres (Fig. 9a). The reflection at 3.7 Å (inter sheet distance between such hydrogen bonded chains (Fig. 9c) corresponds to the distance between the layers of hydrogen bonding planes and distance between benzene groups which are stacked over each other through π – π interaction [44–47]. Based on X-ray diffraction from gel fibres, we conclude that the hydrogen bonding occurs in the direction of growth, and due to the long alkyl chains on either end of the molecules, van der Waals interaction between these side chains also occur along the same direction as the hydrogen bonds, i.e. along the growth direction. The interaction in the direction normal to the growth direction is simply the van der Waals interaction between the terminal methyl groups of the molecules (Fig. 9a). Thus, both hydrogen bonding and van der Waals interactions predominate along the growth direction. However, the relative intensity recorded for a d spacing's of 3.7 and 4.6 Å decreases from BG₈ to BG₁₀ and then increases significantly Table S1 and Fig S7(a). The increase in its intensity with the alkyl chain lengths indicates that side chain packing is enhanced. It is known that the distance between the chains in the polyethylene crystal structure is about 4.5 Å. A reflection with this spacing was also observed in the case of aliphatic polyurethanes and attributed to the distance between the hydrogen bonded chains [48]. It is also noted that the d spacing of the most intense reflection at low angle was found to be 17.2, 21.9, 24.0, 27.0 and 33.4 Å

Fig. 9 **a** Schematic presentation of the molecular aggregation of gelator molecule via N–H···O hydrogen bonds, van der Waals and π – π stackings, **b** fibre formation and **c** stacking of hydrogen bonding planes

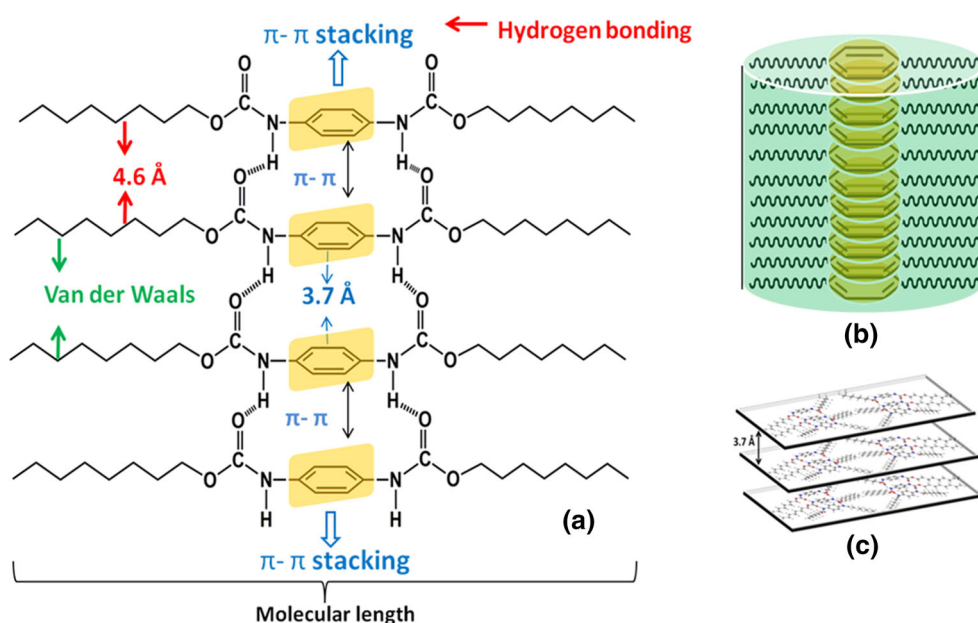
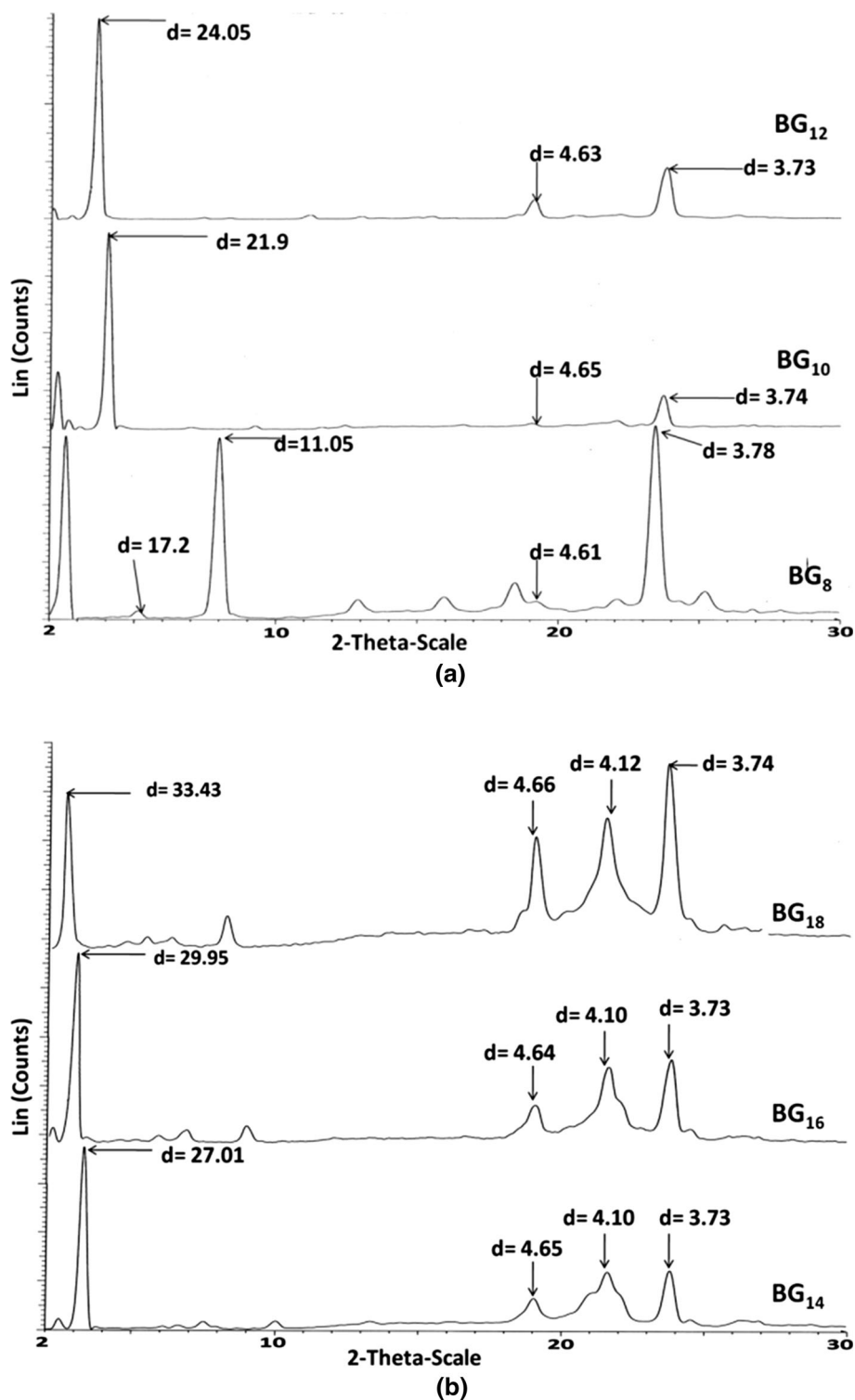


Fig. 10 **a** XRD diffractograms of the xerogels of BG₈–BG₁₂ and **b** XRD diffractograms of the xerogels of BG₁₄–BG₁₈



for BG₈, BG₁₀, BG₁₂, BG₁₄, BG₁₆ and BG₁₈, respectively. This confirmed that the d spacing increases with increasing alkyl chain length. These d spacings arise from the packing of long alkyl chains due to the van der Waals interaction and which match well with the calculated molecular lengths of BG₈–BG₁₈ gelators.

Variation of crystallite size with the alkyl chain length corresponding to the 3.7 and 4.6 Å reflections ($2\theta = 23.4^\circ$ and 19.3° , respectively) for the xerogels is shown in Fig. S7 (b) and Table S2 (supporting information). The crystallite size for $d = 3.7$ Å is almost same for all xerogels but BG₁₀ showing higher crystallite size. However, for $d = 4.6$ Å,

the crystallite size increases significantly from BG₁₄ to BG₁₈. It is difficult to measure the crystallite size of BG₈, BG₁₀ and BG₁₂ at $d = 4.6 \text{ \AA}$ due to low peak intensity. The systems discussed here contain fatty acid chains, and the possibility of Bragg peaks corresponding to the polymorphic forms of fat samples in the WAXS region cannot be ruled out. In a recent Ref. [48], Martinez et al. have discussed the presence of sub- α crystal structure in some monoglycerides of safflower oil solutions. Hence, the characteristic diffraction peaks around 4.6, 4.1 and 3.7 \AA may also arise due to the sub- α crystal structure of the fatty acid residues in the organogelators. This is more significantly seen in BG₁₄, BG₁₆ and BG₁₈, whereas the lower alkyl chain lengths do not show such a diffraction pattern.

4 Conclusions

We have demonstrated the unique self-assembling ability of novel biscarbamate gelators, which showed strong gelation abilities in some organic solvents (e.g. toluene, xylene, NMP and cyclohexanol) resulting in opaque thermoreversible gels. As the alkyl chain length of the biscarbamate was increased incrementally from 8 to 18 carbon atoms, T_{gel} decreased and then increased profoundly from 83 to 105 °C. This could be due to hydrogen bonding predominating at shorter alkyl chain lengths (BG₈), and van der Waals interactions predominating at longer alkyl chain lengths (BG₁₈) of the side chains, and a balance between the two in the intermediate range (BG₁₂). Results from FTIR spectroscopy revealed that hydrogen bonding was the main driving force for the gelation process, and as the alkyl side chain length increased (BG₈–BG₁₈), the van der Waals interactions were more predominant than hydrogen bonding. This is supported by the shifts of the CH₂ frequencies to lower wavelengths and NH frequencies to higher wavelengths with increasing length of the alkyl chain. The cooperation of hydrogen bonds, hydrophobic interactions and the van der Waals interactions majorly decides the self-assembly, and the molecular structure of the alkyl chain length can directly control both the morphology and the macroscopic properties of the gel. Rheological studies confirmed the stability and elastic property of the gels whose strength depended largely on the concentration and chain length. FE-SEM images suggest the different aggregation modes that depend on the structure of the gelator molecule especially chain length due to the predominant van der Waals interaction between the long alkyl chains; in addition to the double hydrogen bonding in biscarbamates, the morphology consists of fibres. We also observed that as alkyl chain length increased the relative attraction (van der Waals forces) of the molecules increased so width of the fibre also increased. It is

concluded that competitive or cooperative interactions of gelator–gelator and solvent–gelator control the morphology of these one-component self-assembled organogel materials. Solid-state UV–visible studies on xerogels showed a clear π – π stacking of benzene rings. From WAXS studies, the packing mode was arrived at and the distance between the plane of hydrogen bonding and inter sheet distance were found to be 4.6 \AA and 3.7 \AA , respectively. BG₁₀ and BG₁₂ xerogels showed less intense peaks in these regions because of their structures deviating from sub- α crystal structure. This behaviour was substantiated by DSC studies carried out on the gels.

Acknowledgments Sravan Baddi is indebted to Council of Scientific and Industrial Research (CSIR), India, for Senior Research Fellowship (SRF).

References

- Philp D, Stoddart JF (1996) Self-assembly in natural and unnatural systems. *Angew Chem Int Ed Engl* 35:1154–1196
- Fuhrhop JH, Köning J (1994) Membranes and molecular assemblies: the synkinetic approach, royal society of chemistry, Cambridge. Royal Society of Chemistry, Cambridge
- Lehn JM (1995) Supramolecular chemistry. VCH, Weinheim
- Ye E, Pei LC, Ankshita P, Xiaotian F, Cally O, Valerie JY, Xian JL (2014) Supramolecular soft biomaterials for biomedical applications. *Mater Today* 17:194–202
- Terech P, Weiss RG (1997) Low molecular mass gelators of organic liquids and the properties of their gels. *Chem Rev* 97:3133–3159
- Jung JH, Lee JH, Silverman JR, John G (2013) Coordination polymer gels with important environmental and biological applications. *Chem Soc Rev* 42:924–936
- Segarra-Maset MD, Nebot VJ, Miravet JF, Escuder B (2013) Control of molecular gelation by chemical stimuli. *Chem Soc Rev* 42:7086–7098
- Moniruzzaman M, Sahin A, Winey KI (2009) Improved mechanical strength and electrical conductivity of organogels containing carbon nanotubes. *Carbon* 47:645–650
- Tew GN, Scott RW, Klein ML, Degrado WF (2010) De novo design of antimicrobial polymers, foldamers, and small molecules: from discovery to practical applications. *Acc Chem Res* 43:30
- Horne WS, Gellman SH (2008) Foldamers with heterogeneous backbones. *Acc Chem Res* 41:1399
- Gellman SH (1998) Foldamers: a manifesto. *Acc Chem Res* 31:173
- Hill DJ, Mio MJ, Prince RB, Hughes TS, Moore JS (2001) A field guide to foldamers. *Chem Rev* 101:3893
- Sanford AR, Yamato K, Yang X, Yuan L, Han Y, Gong B (2004) Well-defined secondary structures. *Eur J Biochem* 271:1416
- Yang X, Martinovic S, Smith RD, Gong B (2003) Duplex foldamers from assembly induced folding. *J Am Chem Soc* 125:9932
- Archer EA, Gong H, Krische MJ (2001) Hydrogen bonding in noncovalent synthesis: selectivity and the directed organization of molecular strands. *Tetrahedron* 57:1139–1159
- Zimmerman SC, Corbin PS (2000) Heteroaromatic modules for self-assembly using multiple hydrogen bonds. *Struct Bonding (Berlin)* 96:63–94

17. Schmuck C, Wienand W (2001) Self-complementary quadruple hydrogen-bonding motifs as a functional principle: from dimeric supramolecules to supramolecular polymers. *Angew Chem Int Ed* 40:4363–4369
18. Khanna S, Moniruzzaman M, Sundararajan PR (2006) Influence of Single versus Double Hydrogen-Bonding Motif on the Crystallization and Morphology of Self-Assembling Carbamates with Alkyl Side Chains: model System for Polyurethanes. *J Phys Chem B* 110:15251–15260
19. Sangeetha NM, Maitra Uday (2005) supramolecular gels: functions and uses. *Chem Soc Rev* 34:821–836
20. Branco MC, Schneider JP (2009) Self-assembling materials for therapeutic delivery. *Acta Biomater* 5:817–831
21. Babu SS, Praveen VK, Ajayaghosh A (2014) Functional π -gelators and their applications. *Chem Rev* 114:1973–2129
22. Srivastava SP, Saxena AK, Tendon RS, Shekhar V (1997) Measurement and prediction of solubility of petroleum waxes in organic solvents. *Fuel* 76:625–630
23. Kanakaiah V, Latha M, Sravan B, Palanisamy Aruna, Vatsala Rani J (2014) Rechargeable magnesium carbon-fluoride battery with electrolyte gel of ionic liquid and low molecular weight gelator. *J Electrochem Soc* 161:A1586–A1592
24. Fernanda PM, Marangoni AG (2009) AOCS official method Cj 2-95 X-ray diffraction analysis of fats. In: Official methods and recommended practices of the AOCS, 6th edn. 2011–2012 Methods and Additions and Revisions
25. DeMan JM, deMan L (2001) Texture of fats. In: Marangoni A, Narine S, Marcel Dekker (eds) Physical properties of lipids, p 191–217. Analytical Methods, Procedures and Theory for the Physical Characterization of Fats Section 1: X-Ray Powder Diffractometry (XRD)
26. Li Yuangang, Liu Kaiqiang, Liu Jing, Peng Junxia, Feng Xuli, Fang Yu (2006) Amino acid derivatives of cholesterol as “latent” organogelators with hydrogen chloride as a protonation reagent. *Langmuir* 22:7016–7020
27. Xue Min, Gao Di, Chen Xiangli, Liu Kaiqiang, Fang Yu (2011) New dimeric cholesteryl-based A (LS) $₂$ gelators with remarkable gelling abilities: organogel formation at room temperature. *J Colloid Interface Sci* 361:556–564
28. Peng Junxia, Liu Kaiqiang, Liu Jing, Zhang Qihong, Feng Xuli, Fang Yu (2008) New dicholesteryl-based gelators: chirality and spacer length effect. *Langmuir* 24:2992–3000
29. Dastidar Parthasarathi (2008) Supramolecular gelling agents: can they be designed. *Chem Soc Rev* 37:2699–2715
30. Rogers MA, Weiss RG (2015) Systematic modifications of alkane-based molecular gelators and the consequences to the structures and properties of their gels. *New J, Chem*
31. Willemsen HM, Vermonden T, Marcelis AT, Sudhölter EJ (2002) Alkyl derivatives of cholic acid as organogelators: one-component and two-component gels. *Langmuir* 18:7102–7106
32. Willemsen HM, Vermonden Tina, Marcelis Antonius, Sudhölter Ernst JR (2001) N-Cholyl amino acid alkyl Esters-A novel class of organogelators. *EJOC* 12:2329–2335
33. Sravan B, Kamalakar K, Karuna MSL, Palanisamy Aruna (2014) Studies on organogelation of self-assembling bis urea type low molecular weight molecules. *J Sol-Gel Sci Technol* 71:372–379
34. Delbecq F, Masuda Y, Ogue Y, Kawai T (2012) Salt complexes of two-component N-acylamino acid diastereoisomers: self-assembly studies and modulation of gelation abilities. *Tetrahedron Lett* 53:6588–6593
35. Ducouret G, Chassenieux C, Martins S, Lequeux F, Bouteiller L (2007) Rheological characterisation of bis-urea based viscoelastic solutions in an apolar solvent. *J Colloid Interface Sci* 310:624–629
36. Isare B, Bouteiller L, Ducouret G, Lequeux F (2009) Tuning reversible supramolecular polymer properties through co-monomer addition. *Supramol Chem* 21:416–421
37. Ajish JK, Kumar KA, Subramanian M, Kumar M (2014) D-Glucose based bisacrylamide crosslinker: synthesis and study of homogeneous biocompatible glycopolymeric hydrogels. *RSC Adv* 4:59370–59378
38. Pal A, Mahapatra RD, Dey J (2014) Understanding the role of H-bonding in self-aggregation in organic liquids by fatty acid amphiphiles with a hydrocarbon tail containing different H-bonding linker groups. *Langmuir* 30:13791–13798
39. Wuerthner F, Bauer C, Stepanenko V, Yagai SA (2008) Black perylene bisimide super gelator with an unexpected J-type absorption band. *Adv Mater* 20:1695–1698
40. Chung JW, An BK, Park SYA (2008) Thermoreversible and proton-induced gel – sol phase transition with remarkable fluorescence variation. *Chem Mater* 20:6750–6755
41. Würthner F, Thalacker C, Diele S, Tschierske C (2001) Fluorescent J-type aggregates and thermotropic columnar mesophases of perylene bisimide dyes. *Chem Eur J* 7:2245–2253
42. Shirakawa M, Kawano SI, Fujita N, Sada K, Shinkai S (2003) Hydrogen-bond-assisted control of H versus J aggregation mode of porphyrins stacks in an organogel system. *J Org Chem* 68:5037–5044
43. Bai B, Mao X, Wei J, Wei Z, Wang H, Li M (2015) Selective anion-responsive organogel based on a gelator containing hydrazide and azobenzene units. *Sens Actuator B-Chem* 211:268–274
44. Ajayaghosh A, Praveen VK (2007) π -Organogels of self-assembled p-phenylenevinylenes: soft materials with distinct size, shape, and functions. *Acc Chem Res* 40:644–656
45. Dhinakaran MK, Sundarajan K, Das TM (2014) Synthesis of novel benzimidazole-carbazole-N-glycosylamines and their self-assembly into nanofibers. *New. J Chem* 38:4371–4379
46. Huang YD, Tu W, Yuan YQ, Fan DL (2014) Novel organogelators based on pyrazine-2, 5-dicarboxylic acid derivatives and their mesomorphic behaviors. *Tetrahedron* 70:1274–1282
47. Alimova LL, Atovmyan EG, Filipenko OS (1987) The crystal and molecular-structure of hexamethylene-1, 6-(0, 0'-didecyl)-diurethane. *Kristallografiya* 32:97–101
48. López-Martínez A, Morales-Rueda JA, Dibildox-Alvarado E, Charó-Alonso MA, Marangoni AG, Toro-Vazquez JF (2014) Comparing the crystallization and rheological behavior of organogels developed by pure and commercial monoglycerides in vegetable oil. *Food Res Int* 64:946–957